Martian pedestal craters: Marginal sublimation pits implicate a climate-related formation mechanism

Seth J. Kadish,[1] James W. Head,[1] Nadine G. Barlow,[2] and David R. Marchant[3]

[1] Pedestal craters on Mars are defined by an outward-facing scarp forming a plateau perched tens of meters above the surrounding terrain. Their origin has been attributed to impact armoring of the surface and subsequent removal of inter-crater terrain by either eolian deflation or sublimation of an ice-rich substrate. We identified 2696 pedestal craters between ~60°N and 60°S latitude; 98% are poleward of 33°N and 40°S. The majority of pedestal crater margins are smoothly sloped, but ~3%, concentrated in Utopia Planitia and Malea Planum, display distinctive marginal pits. These pedestal crater scarps are anomalously tall (usually >80–100 m) and the pits resemble sublimation depressions seen on Earth and elsewhere on Mars, providing evidence for sublimation of volatiles in the scarp, where the armored surface has tapered. The pitted scarps provide insight into the origin of the general pedestal crater population, favoring formation via deposition of a volatile-rich substrate, impact armoring, and sublimation of intervening volatiles. Crater densities and overlapping pedestal craters suggest multiple periods of emplacement and loss of these climate-related, latitude-dependent deposits throughout the Amazonian. **Citation:** Kadish, S. J., J. W. Head, N. G. Barlow, and D. R. Marchant (2008), Martian pedestal craters: Marginal sublimation pits implicate a climate-related formation mechanism, *Geophys. Res. Lett.*, *35*, L16104, doi:10.1029/2008GL034990.

1. Introduction

[2] Pedestal craters are a subclass of impact craters unique to Mars [*Barlow et al.*, 2000] characterized by a crater perched near the center of a pedestal (mesa or plateau) that is surrounded by an often-circular, outward-facing scarp (Figures 1 and 2). The pedestal radius is large compared to the expected ejecta radius, with the scarp several crater diameters from the rim crest, and elevated tens to over 100 meters above the surrounding terrain. Hypotheses for pedestal crater formation suggested that the substrate was armored during the impact event (see *Wrobel et al.* [2006] for summary of suggested mechanisms) and protected from subsequent erosion that removed the surrounding substrate. Proposals for the armored surface material include ejecta deposits, a coarse lag deposit, a veneer of impact melt, or a thermally indurated soil consisting of a layer of fine-grained, volatile-poor dust. Following armoring, a marginal scarp is created by preferential erosion of the substrate surrounding the armored region, most commonly thought to involve eolian deflation of fine-grained, unarmored material [e.g., *Arvidson et al.*, 1976], or preferential removal of a volatile-rich, climate-related substrate by sublimation [e.g., *Kadish and Barlow*, 2006]. Here we report on the detection of features interpreted to be sublimation pits along the margins of pedestal craters in each hemisphere. These pits provide evidence for the presence of ice and snow underlying the pedestal surface.

2. Distribution of Pitted Pedestal Craters

[3] In order to test various hypotheses for the origin of pedestal craters, *Kadish and Barlow* [2006] mapped 2696 pedestal craters with diameters >0.7 km equatorward of ~60°N and S latitude (Figure 1). Pedestal craters are not distributed randomly, occurring in the northern hemisphere almost exclusively poleward of 33°N, with the majority between 45° and 60°N. In the southern hemisphere they are four times less abundant, and occur almost exclusively poleward of 40°S. Their distribution is latitude-dependent and similar to 1) ice currently in the substrate [*Boynton et al.*, 2002], 2) surface roughness data suggesting smoothing by emplacement of a meters to tens-of-meters thick mantle [*Kreslavsky and Head*, 2000], 3) a host of geomorphic features (e.g. ice-rich mantle, polygons, viscous flow features, dissected terrain) interpreted to represent the deposits from a recent ice age [*Mustard et al.*, 2001], and 4) a wide range of ice-related features interpreted to represent deposition of ice and snow driven by climate change [*Head et al.*, 2003; *Head and Marchant*, 2008].

[4] We found that 71 pedestal craters exhibited one or more pits along the pedestal margin. Pitted pedestal craters are not evenly distributed in the latitude bands where most pedestal craters form (Figure 1), instead occurring in two concentrations: 51 in the northern hemisphere (Utopia Planitia) and 20 in the southern hemisphere (Malea Planum). The search for pedestal craters with pits was extended to 70°N and S latitude to improve our understanding of their geographic extent. All pitted pedestal craters are poleward of 48°N and 55°S latitude (Figure 1). Here we explore the significance of pedestal craters with pitted margins for understanding the nature of the substrate.

3. Description of Pitted Pedestal Craters

[5] Pitted pedestal craters (Figures 2 and 3) are perched an average of ~100 m above surrounding plains (Figures 2h and 2i); non-pitted pedestals are usually elevated only ~50 m [*Kadish et al.*, 2008; also Latitude dependence of Martian pedestal craters: Evidence for a sublimation-driven

[1]Department of Geological Sciences, Brown University, Providence, Rhode Island, USA.
[2]Department of Physics and Astronomy, Northern Arizona University, Flagstaff, Arizona, USA.
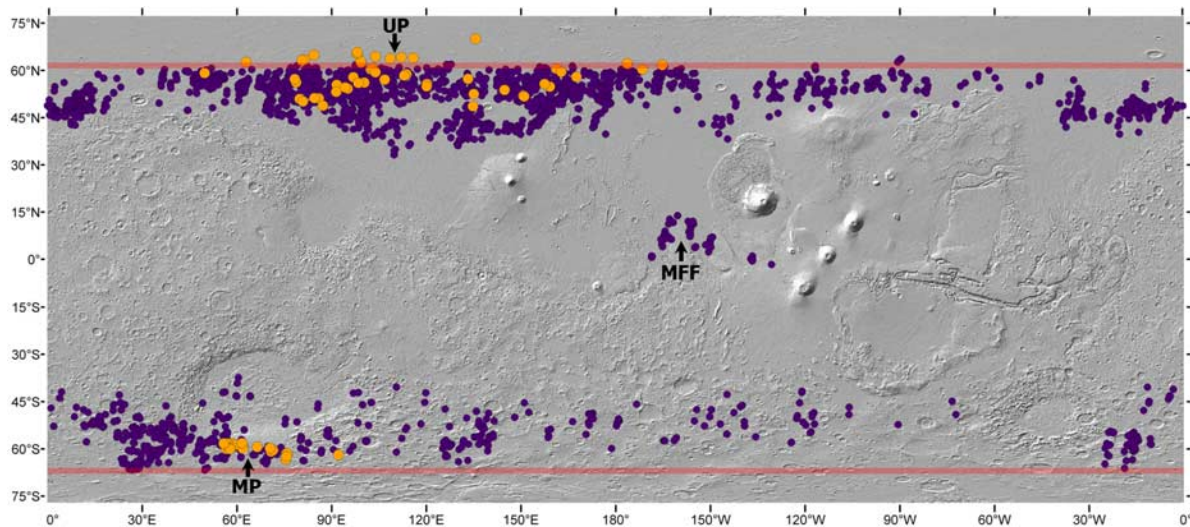[3]Department of Earth Sciences, Boston University, Boston, Massachusetts, USA.

Figure 1. The distribution of pedestal craters (purple circles) on Mars between ∼60°N and 65°S (red lines). Pedestal with marginal pits (orange circles) are concentrated in Utopia Planitia (UP) and Malea Planum (MP). The only equatorial pedestal craters were detected in the Medusae Fossae Formation (MFF).

formation mechanism, manuscript in preparation, 2008]. In pitted cases, the marginal scarp at the pedestal plateau edge slopes down to the surrounding terrain, except where it is interrupted by a pit (Figures 2a–2d). Individual pits are characterized by cuspate shapes and alcove-like features, especially along the perimeter proximal to the crater; the distal portions of the pit rims are often sinuous, but lack alcove-like features (Figures 2e–2g). The pits have a typical depth of ∼20 m (Figures 2h and 2i) and can form in any orientation around the circumference of the scarp (Figures 2a–2d and 3a); we saw no significant pole-facing or equator-facing trend for pits. Altimetry data indicate that pits form at the pedestal margin, rather than in the adjacent surrounding terrain, and they do not extend to depths lower than the elevation of the surrounding substrate (Figures 2h–2i and 3b). MOLA data suggest that pit interior slopes are generally shallow, and do not exceed ∼10°. Pit slopes have minimal variability around the perimeter of the pit, with no pit wall orientation appearing typically steeper. Pits are usually elongated along the pedestal crater scarp and often appear to coalesce to form larger pits, resulting in marginal depressions that extend along a significant part of the pedestal circumference (Figures 2a and 3a).

[6] A detailed depiction of a ∼3.9 km-diameter pitted pedestal crater shows that it is centered on a plateau perched ∼100 m above the adjacent plains (Figure 2). The planform of the pedestal is roughly circular, with a lobe extending to the northeast (Figure 2a). The pedestal surface is extremely flat, with slopes <1° in the area between the crater rim and the marginal scarp; perspective views (Figures 2b–2d) show that even at a vertical exaggeration of 15x, the armored pedestal surface is remarkably smooth. While marginal pits dot almost the entire circumference of the scarp, the largest pits are concentrated on the south and east-facing slopes (Figure 2a and 2e–2g). These pits are generally 1–3 km in length (measured tangential to the marginal scarp), and <2 km in width (measured normal to the scarp).

[7] Some pitted pedestal craters (Figure 3a) exhibit a series of coalesced marginal pits that together form a moat-

like structure that can trace a significant portion of the pedestal margin. Although they are longer, these pits have similar widths (∼1 km) and depths (∼20 m) to the pits in Figure 2. The bowl of the 2.5-km-diameter impact crater in Figure 3a is at an elevation similar to that of the pedestal surface, with the crater rim extending ∼20–30 m above the pedestal (Figure 3b). This pedestal is circular, sloping <1° toward the west; the eastern margin of the pedestal is contiguous with a bordering unit, which has a N–S trending scarp, elevating it ∼180 m above the plains. In some cases, pedestal craters are superposed on each other. In Figure 3c, the younger pedestal is clearly draped over the older pedestal, suggesting two different episodes of pedestal crater formation, separated by the loss of the intervening inter-crater deposits.

[8] Some pits contain small isolated mesas (Figures 2e–2g), whereas others appear to be smooth, uninterrupted depressions. These isolated mesas vary in size, shape, and orientation; the margins of each mesa commonly mimic the curvatures of the encompassing pit rims (Figures 2e–2g). Mesa tops are smoother than adjacent pit floors and typically match the texture of the surrounding pedestal surface. In at least one case (Figure 2e, left) the mesa surface grades evenly with the surrounding pedestal surface. MOLA data (Figure 2i) confirm that the mesas maintain the original slopes of the pedestal margins; they have not lowered in elevation like the surrounding pit surface.

4. Discussion, Interpretation and Implications for Pedestal Crater Formation

[9] Pits associated with pedestal craters are similar in morphology to features interpreted to represent the subli-mation of ice in many different environments in the solar system [Moore et al., 1996], including Mars (dissected terrain [Mustard et al., 2001; Head et al., 2003]; pits on the floors of some outflow channels [Levy and Head, 2005]; outwash plains and thermokarstic regions [Costard and Kargel, 1995]; formerly ice-rich and now beheaded pits in
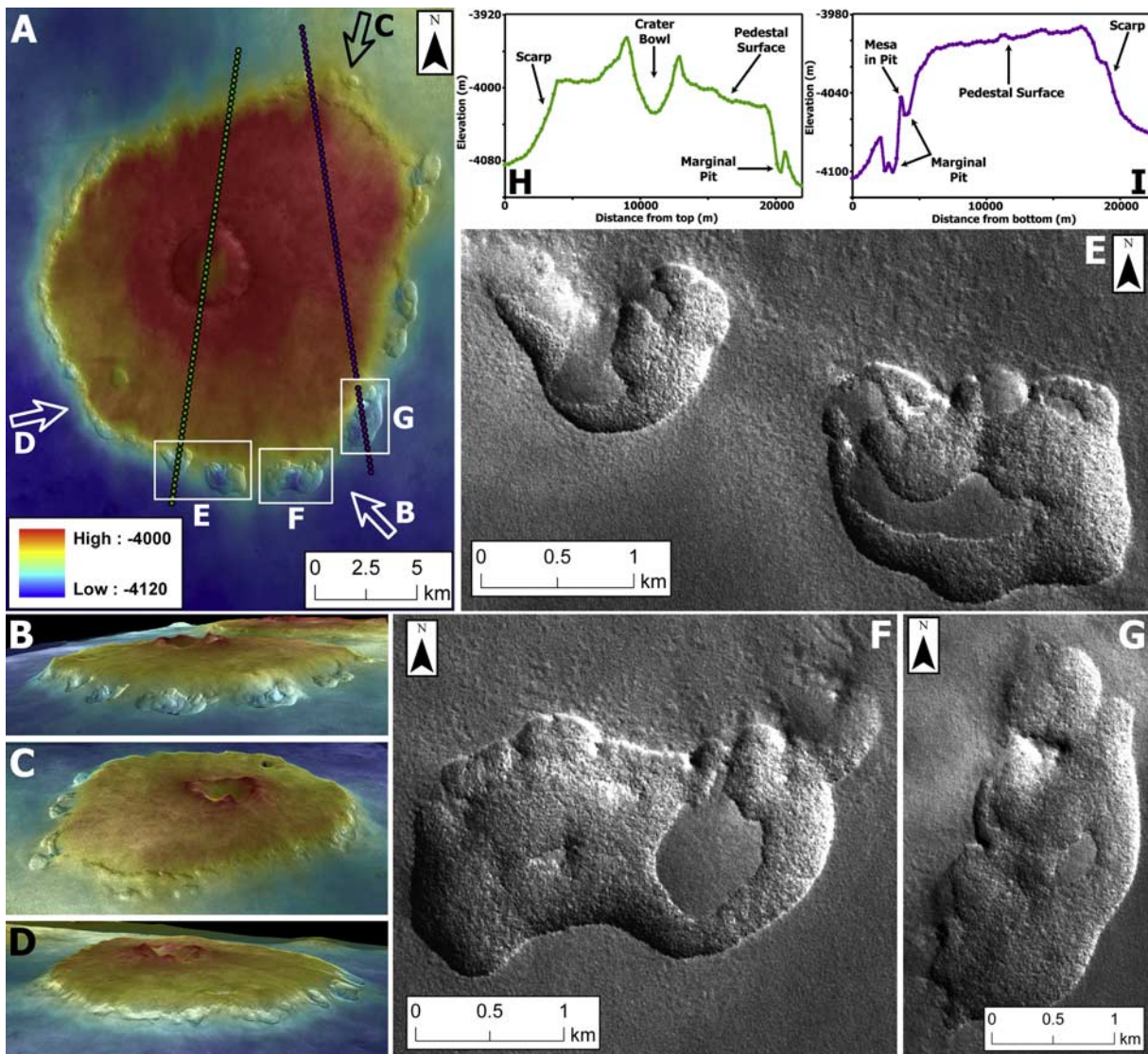
Figure 2. (a) A pedestal crater with marginal pits (CTX image P01_001555_2430 overlain on MOLA altimetry data; 62.4°N, 99.4°E). (b)−(d) Perspective views (VE = 15x), showing that the location of the pits is in the pedestal scarp, rather than the surrounding terrain. (e)−(g) Enlarged sections, displaying detailed pit morphology. Illumination is from the left. (h)−(i) Topographic profiles across the pedestal in Figure 2a. The depth of the pits does not exceed the elevation of the surrounding terrain.

the proximal part of debris-covered glaciers [*Marchant and Head*, 2007]; flat-floored, quasi-circular depressions with steep sides known as Swiss cheese features in the south-polar residual cap [*Thomas et al.*, 2000]). For example, a similar pit morphology exists in western Utopia Planitia (Figure 4), just south of the population we have identified, and is interpreted to be due to sublimation and thermokarstic processes [*Costard and Kargel*, 1995; *Morgenstern et al.*, 2007; *Lefort et al.*, 2007]. These morphologically fresh, rimless pits occur in the surrounding substrate, but have similar characteristics and depths to pits in pedestal scarps. Scallops and pits are also found in Malea Planum (Figure 4) in plains between pitted pedestal craters [*Lefort et al.*, 2005, 2006; *Zanetti et al.*, 2008]. The scallops and pits are 5−20 m deep, and are interpreted to be due to sublimation of ice from a climate-related, ice-rich, mantling layer. The simi-

larity of these features in their geomorphology and geographic location strengthens the interpretation of pits in pedestal crater scarps as being related to ice-rich layers associated with climate change. In this case, localized volatile loss via sublimation physically removes volume from the substrate at the pedestal scarp, resulting in the growth of a pit as the material remaining at the pedestal margin depresses and settles. The formation of pits in some pedestal craters and not others is likely related to the increased heights of some pedestal crater scarps. Pitted pedestal craters are characterized by steeper and more extensive marginal slopes, favoring downslope movement, shedding of the overlying protective regolith, and exposure of the underlying volatile substrate to enhanced insolation. The isolated mesas in pits therefore represent regions where remnant armoring material is inhibiting sublimation, yield-
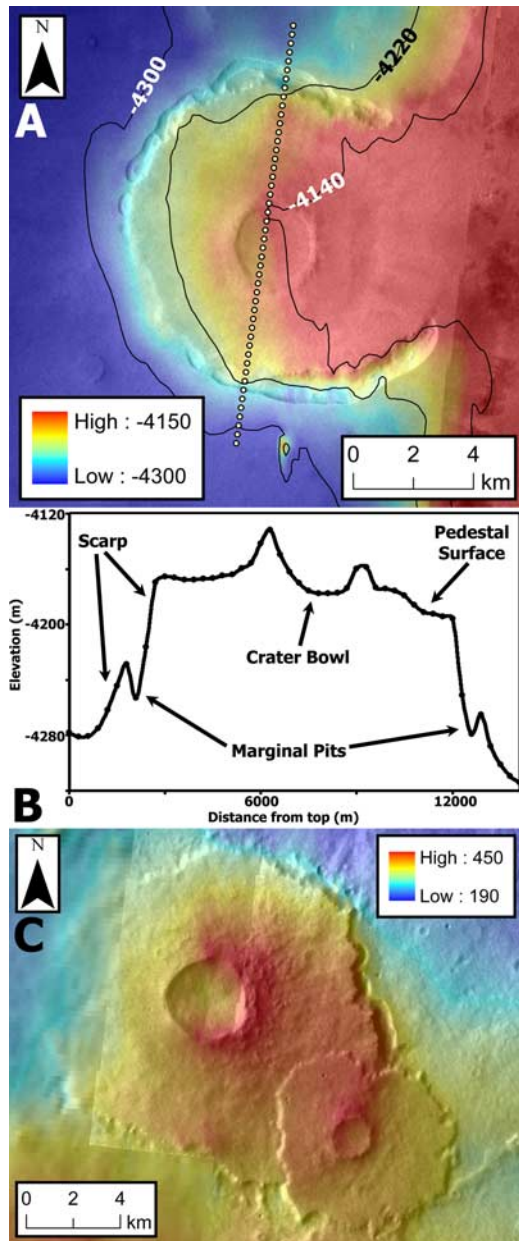
Figure 3. (a) A pedestal crater with marginal pits that have coalesced to form a moat-like structure (subscene of THEMIS image V10457014; 60.2°N, 102.5°E). (b) Altimetry profile across the pedestal crater in Figure 3a. (c) One pedestal partially draped over another (THEMIS mosaic; 61.3°S, 71.2°E). The larger pedestal has developed marginal pits, one of which is truncated by the smaller pedestal. This superposition relationship suggests that pedestals did not all form from the same ice-rich mantle; rather they formed during multiple periods of mantle emplacement and removal.

ing localized preservation of the underlying substrate. The distinctive latitudinal-dependence of the general pedestal crater distribution (Figure 1), and their correlation with other mid- to high-latitude deposits interpreted to be related to deposition of volatiles during Amazonian climatic excursions [e.g., see *Head and Marchant*, 2008], suggests that similar climate-related processes of deposition and removal

of volatiles are involved in their origin [*Kadish et al.*, 2008, manuscript in preparation, 2008].

[10] Why are pitted pedestal craters concentrated in two groupings (Figure 1) in the northern and southern hemisphere? The anomalous heights of the pitted pedestal craters suggest that the underlying substrate that existed at the time of crater formation was a factor of two thicker than in other regions of pedestal crater formation. Although deposition of snow and ice during periods of climate change in the past history of Mars may have generally followed a broad latitudinal distribution [*Head and Marchant*, 2008], there is ample evidence for local variations as well. For example, *Forget et al.* [2006] performed high-resolution climate simulations with a model that includes the current water cycle and assumes a spin-axis obliquity of 45°. These simulations predict significant preferential ice accumulation from a south polar water source that operates efficiently at southern summer solstice when the southern polar cap releases large amounts of water vapor. This water vapor moves northward and is deflected by cold air moving southward from the Hellas basin toward Malea Planum; the subsequent cooling causes strong condensation and precipitation in the Hellas region. In the northern hemisphere, *Madeleine et al.* [2007] examined meteorological conditions during periods of moderate obliquity and high dust loading and found that the resulting climate favors formation of a thick cloud belt with significant ice precipitation and accumulation, particularly in western Utopia Planitia. We thus conclude that the non-pitted pedestal
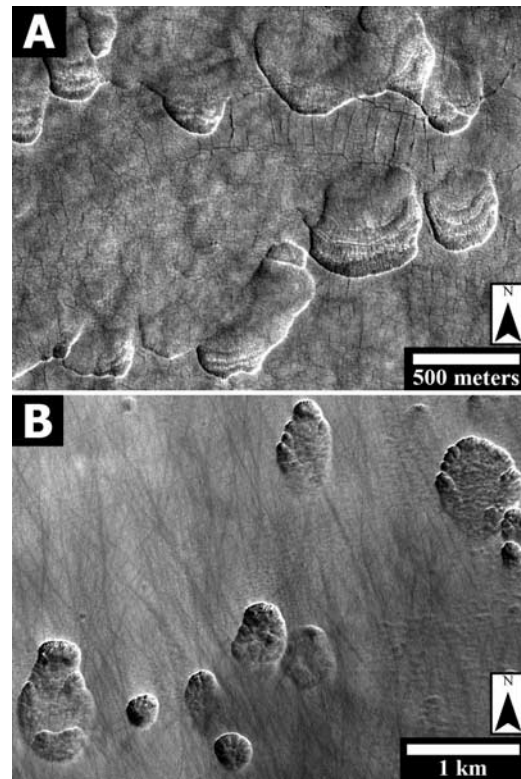

Figure 4. Scalloped terrain interpreted to form via sublimation in (a) Utopia Planitia (subscene of HiRISE image PSP_001331_2260) and (b) Malea Planum (subscene of HiRISE image PSP_004168_1220). Illumination is from top left in Figure 4a and bottom left in Figure 4b.

craters represent formation in regional climate-dependent, volatile-rich deposits, while pitted pedestal craters formed in local regions of enhanced precipitation and accumulation.

[11] On the basis of the evidence gathered, we propose the following formation mechanism for all pedestal craters: An impact occurs into fine-grained, ice-rich material emplaced during a period of high obliquity. The surface surrounding the impact becomes armored via a shock wave in the form of an atmospheric blast followed by a high-temperature thermal pulse. These atmospheric effects cause melting and migration of the ice in the top several centimeters of the volatile-rich, climate-related deposit. Removing the ice fraction from the near-surface produces a protective soil layer composed of fine-grained, volatile-poor dust [*Wrobel et al.*, 2006]. We prefer this armoring mechanism because it is capable of indurating the surface to a lateral extent greater than the edge of the continuous ejecta deposit, which explains the anomalously large radii of the pedestals. As conditions change during return to low obliquity, volatiles sublimate from the unarmored inter-crater terrain. The loss of volume results in a lowering of the elevation of the plains, causing a scarp to form at the edge of the armored crater, yielding the pedestal. Armoring inhibits sublimation from beneath the pedestal surface, leaving the pedestal perched above a locally ice-rich sub-strate. As sublimation occurs at the edge of the armored surface, it creates the debris-covered, marginal pedestal slopes. For most pedestal craters, an equilibrium between sublimation and debris cover is reached, stabilizing the margin of the pedestal. In anomalously tall pedestal craters, the slopes are preferentially mass-wasted and sublimation and loss of volatiles produces marginal pits in the scarp, which can reach depths only as great as the vertical extent of the ice-rich deposit. As such, pits cannot excavate to depths lower in elevation than the surrounding volatile-poor terrain, in agreement with observations (Figures 2 and 3).

5. Conclusions

[12] Pits along the marginal scarps of some pedestal craters provide geomorphic evidence for sublimation of volatiles from the substrate underlying the armored pedestal surface. Pedestal craters are thus interpreted to represent the remnants of a once much more extensive, high-latitude, ice-rich climate-related deposit, similar to, but much thicker than the layered latitude-dependent mantle emplaced during a recent ice age [*Mustard et al.*, 2001; *Head et al.*, 2003]. The large number and widespread nature of pedestal craters [*Kadish and Barlow*, 2006] means that this climate-related deposit persisted for a substantial part of the recent past, implying that obliquity was relatively higher than at present during extended periods in the Amazonian. Superposed pedestal craters (Figure 3c) suggest that these conditions recurred.

References

Arvidson, R. E., M. Coradini, A. Carusi, A. Coradini, M. Fulchignoni, C. Federico, R. Funiciello, and M. Salomone (1976), Latitudinal variation of wind erosion of crater ejecta deposits on Mars, *Icarus*, 27, 503–516.

Barlow, N. G., J. M. Boyce, F. M. Costard, R. A. Craddock, J. B. Garvin, S. E. H. Sakimoto, R. O. Kuzmin, D. J. Roddy, and L. A. Soderblom (2000), Standardizing the nomenclature of Martian impact crater ejecta morphologies, *J. Geophys. Res.*, 105, 26,733–26,738.

Boynton, W. V., et al. (2002), Distribution of hydrogen in the near surface of Mars: Evidence for subsurface ice deposits, *Science*, 297, 81–85.

Costard, F. M., and J. S. Kargel (1995), Outwash plains and thermokarst on Mars, *Icarus*, 114, 93–112.

Forget, F., R. M. Haberle, F. Montmessin, B. Levrard, and J. W. Head (2006), Formation of glaciers on Mars by atmospheric precipitation at high obliquity, *Science*, 311, 368–371.

Head, J. W., and D. R. Marchant (2008), Evidence for non-polar ice deposits in the past history of Mars, *Lunar Planet. Sci. [CD-ROM]*, XXXIX, Abstract 1295.

Head, J. W., J. F. Mustard, M. A. Kreslavsky, R. E. Milliken, and D. R. Marchant (2003), Recent ice ages on Mars, *Nature*, 426, 797–802.

Kadish, S. J., and N. G. Barlow (2006), Pedestal crater distribution and implications for a new model of formation, *Lunar Planet. Sci. [CD-ROM]*, XXXVII, Abstract 1254.

Kadish, S. J., J. W. Head, and N. G. Barlow (2008), Pedestal craters on Mars: Distribution, characteristics, and implications for Amazonian climate change, *Lunar Planet. Sci. [CD-ROM]*, XXXIX, Abstract 1766.

Kreslavsky, M. A., and J. W. Head (2000), Kilometer-scale roughness of Mars: Results from MOLA data analysis, *J. Geophys. Res.*, 105, 26,695–26,712.

Lefort, A., P. Russell, and N. Thomas (2005), Ice sublimation landforms in Peneus and Amphitrites Patera, *Lunar Planet. Sci. [CD-ROM]*, XXXVI, Abstract 1626.

Lefort, A., P. Russell, and N. Thomas (2006), Scallop-shaped depressions and mantle sublimation in the mid-latitudes of Mars, paper presented at Fourth International Conference on Mars Polar Science and Exploration, Lunar and Planet. Inst., Davos, Switzerland.

Lefort, A., P. Russell, N. Thomas, and the HiRISE Team (2007), Scalloped terrains in Utopia Planitia, insight from HiRISE, *Lunar Planet. Sci. [CD-ROM]*, XXXVIII, Abstract 1796.

Levy, J. S., and J. W. Head (2005), Evidence for remnants of ancient ice-rich deposits: Mangala Valles outflow channel, Mars, *Terra Nova*, 17, 503–509.

Madeleine, J. B., F. Forget, J. W. Head, B. Levrard, and F. Montmessin (2007), Mars: A proposed climatic scenario for northern mid-latitude glaciation, *Lunar Planet. Sci. [CD-ROM]*, XXXVIII, Abstract 1778.

Marchant, D. R., and J. W. Head (2007), Antarctic dry valleys: Microclimate zonation, variable geomorphic processes, and implications for assessing climate change on Mars, *Icarus*, 192, 187–222.

Moore, J. M., M. T. Mellon, and A. P. Zent (1996), Mass wasting and ground collapse in terrains of volatile-rich deposits as a solar system–wide geological process: The Pre-Galileo view, *Icarus*, 122, 63–78.

Morgenstern, A., E. Hauber, D. Reiss, S. van Gasselt, G. Grosse, and L. Schirrmeister (2007), Deposition and degradation of a volatile-rich layer in Utopia Planitia and implications for climate history on Mars, *J. Geophys. Res.*, 112, E06010, doi:10.1029/2006JE002869.

Mustard, J. F., C. D. Cooper, and M. K. Rifkin (2001), Evidence for recent climate change on Mars from the identification of youthful near-surface ground ice, *Nature*, 412, 411–414.

Thomas, P. C., M. C. Malin, K. S. Edgett, M. H. Carr, W. K. Hartmann, A. P. Ingersoll, P. B. James, L. A. Soderblom, J. Veverka, and R. Sullivan (2000), North-south geological differences between the residual polar caps on Mars, *Nature*, 404, 161–164.

Wrobel, K., P. H. Schultz, and D. Crawford (2006), An atmospheric blast/thermal model for the formation of high-latitude pedestal craters, *Meteorit. Planet. Sci.*, 41, 1539–1550.

Zanetti, M., H. Hiesinger, D. Reiss, E. Hauber, and G. Neukum (2008), Scalloped depressions in Malea Planum, southern Hellas Basin, Mars, *Lunar Planet. Sci. [CD-ROM]*, XXXIX, Abstract 1682.

———————————

N. G. Barlow, Department of Physics and Astronomy, Northern Arizona University, Flagstaff, AZ 86011, USA.

J. W. Head and S. J. Kadish, Department of Geological Sciences, Brown University, Providence, RI 02912, USA. (james_head@brown.edu)

D. R. Marchant, Department of Earth Sciences, Boston University, Boston, MA 02215, USA.